

## **Disclaimer Statement**

"The contents of this report reflect the views of the author(s) who is (are) responsible for the facts and the accuracy of the data presented herein. The contents do not necessarily reflect the official views or policies of the New Jersey Department of Transportation or the Federal Highway Administration. This report does not constitute a standard, specification, or regulation."

The contents of this report reflect the views of the authors, who are responsible for the facts and the accuracy of the information presented herein. This document is disseminated under the sponsorship of the Department of Transportation, University Transportation Centers Program, in the interest of information exchange. The U.S. Government assumes no liability for the contents or use thereof.

1. Report No. <b>FHWA 1998 - 010</b>		2. Government Accession No.		3. Recipient's Catalog No.	
4. Title and Subtitle <b>Fatigue Performance Of Variable Message Sign &amp; Luminaire Support Structures Volume II - Fatigue Testing and Failure Analysis of Aluminum Luminaire Support Structures</b>				5. Report Date <b>May 1998</b>	
				6. Performing Organization Code <b>CAIT/Rutgers/ATLSS/Lehigh</b>	
7. Author(s) <b>Gary R. Consolazio, Kevin W. Johns, and Robert J. Dexter</b>				8. Performing Organization Report No. <b>FHWA 1998 - 010</b>	
9. Performing Organization Name and Address <b>New Jersey Department of Transportation CN 600 Trenton, NJ 08625</b>				10. Work Unit No.	
				11. Contract or Grant No.	
12. Sponsoring Agency Name and Address <b>Federal Highway Administration U.S. Department of Transportation Washington, D.C.</b>				13. Type of Report and Period Covered <b>Final Report 09/13/1996 - 6/30/1998</b>	
				14. Sponsoring Agency Code	
15. Supplementary Notes					
16. Abstract <p>In Order to determine equivalent static pressures for fatigue loads on cantilevered highway support structures a cantilevered Variable Message Sign(VMS) located along Interstate westbound at mile marker 48.5 in northern New Jersey was continuously monitored for three months. The structure was instrumented with strain gages, pressure transducers, and a wind sentry. All the data was collected with a Campbell Scientific CR9000 digital data acquisition system. A cellular phone transceiver enabled remote communication with the data logger. The system and instrumentation was powered with solar powers and marine batteries. Short-term testing was performed on the structure to determine the dynamic characteristics such as stiffness, natural frequency, and percent of critical damping. Results of the short-term test indicated that the stiffness was 0.24 kN/mm, the first and the second modes were 0.87 cycles/s and 1.22 cycles/s respectively, and the percent of critical damping for the first and second modes were 0.57 percent and 0.25 percent respectively. Long-Term monitoring was performed to capture the structures response to natural wind gusts, galloping, and truck-induced wind gusts. This data would then be used to determine appropriate fatigue design wind loads for future sign support structures. During the three months of monitoring the structure did not experience galloping, which is a phenomena highly dependent on location. A galloping design pressure of 1000 Pa was recommended based on previous research. The summer months, which is when the structure was monitored, were not conducive to the strongest natural winds patterns in Northern New Jersey. The highest natural wind speed that was recorded was 7.5m/s. It is believed that much stronger winds are present in winter and spring, therefore a natural wind gust design pressure of 250 Pa was recommended. Truck-induced gusts were measured and a linear gradient for the truck-induced gust design pressure was determined. The truck-induced gust design pressure ranged linearly from 1760 Pa at 0 to 6m above the surface of the road to 0 Pa at 10.1m and over.</p>					
17. Key Words <b>fatigue, failure analysis, loads, highway, support structures, cantilever, VMS</b>			18. Distribution Statement		
19. Security Classif. (of this report) <b>Unclassified</b>		20. Security Classif. (of this page) <b>Unclassified</b>		21. No of Pages <b>76</b>	22. Price



**LEHIGH**  
University

---

---

# **FATIGUE TESTING AND FAILURE ANALYSIS OF ALUMINUM LUMINAIRE SUPPORT STRUCTURES**

**Final Report**

by

**Kevin W. Johns**  
Graduate Research Assistant  
Lehigh University

**Robert J. Dexter**  
Associate Professor of Civil Engineering  
University of Minnesota

Prepared for:  
New Jersey Department of Transportation  
CN615  
Trenton, New Jersey 08625-0615

**ATLSS Report No. 98-06**  
May 1998

**ATLSS is a National Center for Engineering Research  
on Advanced Technology for Large Structural Systems**

117 ATLSS Drive  
Bethlehem, PA 18015-4729

Phone: (610)758-3535  
Fax: (610)758-5553

[www.lehigh.edu/~inatl/inatl.html](http://www.lehigh.edu/~inatl/inatl.html)  
Email: [inatl@lehigh.edu](mailto:inatl@lehigh.edu)

## **Acknowledgments**

The research reported herein was performed at the Center for Advanced Technology for Large Structural Systems (ATLSS) at Lehigh University. The project was sponsored by the New Jersey Department of Transportation. The authors would like to acknowledge Professor John W. Fisher for providing invaluable guidance over the course of the research program. Robert Connor assisted with the instrumentation, data acquisition and field testing throughout the duration of the project. Ed Tomlinson assisted in the instrumentation and data acquisition process. John Hoffner, Larry Heffner, Steve Leonard, Roger Moyer, Todd Anthony and other ATLSS technicians provided assistance with all laboratory work.

## **Table of Contents**

List of Tables	iv
List of Figures	v
<b>Chapter 1 - Introduction</b>	<b>1</b>
1.1 Problem	1
1.2 Purpose	2
1.3 Scope	2
<b>Chapter 2 - Background</b>	<b>7</b>
2.1 Wind Loading Phenomena Relevant to Luminaires	7
2.1.1 Natural Wind Gusts	7
2.1.2 Vortex Shedding	9
2.1.2.1 Straight Support Standards Susceptibility to Vortex Shedding	10
2.1.2.2 Cantilevered Support Standards Susceptibility to Vortex Shedding	12
2.1.2.3 Recommended Vortex Shedding Design Loads	13
2.2 Background Relevant to Fatigue Resistance of Details	14
<b>Chapter Three: Testing and Findings</b>	<b>29</b>
3.1 History of the New Jersey Luminaire Support Standards	29
3.2 Pull Test Description	30
3.2.1 Cantilevered Support Standards Pull Test Results	30
3.2.2 Straight Support Standards Pull Test Results	31
3.3 Fatigue Test Procedure	32
3.4 Fatigue Test Results	33
3.4.1 Transformer Bases	33
3.4.2 Pole Cracks Induced by Bending	34
3.4.3 Pole Cracks Induced by Shear	35
3.5 Comparison with Route 147 Failures	35
<b>Chapter 4: Conclusions and Recommendations</b>	<b>54</b>
4.1 Conclusions from Fatigue Testing	54
4.2 Design Recommendations	54
4.2.1 Natural Wind Gusts	54
4.2.2 Vortex Shedding	55
4.2.3 Improved Shoe Base-to-Pole Connection	56
4.2.4 Installation Procedure	56
<b>References</b>	<b>57</b>
<b>Appendix A – Fatigue Design Example</b>	<b>59</b>

## **List of Tables**

Table 2-1 Straight Support Standard Modal Analysis Chart.	11
Table 2-2 Cantilevered Support Standard Modal Analysis Chart	13
Table 3-1 Support Standard Fatigue Test Summary	33

## **List of Figures**

Figure 1-1 Cantilevered Luminaire Support Structure.	3
Figure 1-2 Straight Luminaire Support Structure.	4
Figure 1-3 Shoe Base to Pole Connection.	5
Figure 1-4 Transformer Base.	6
Figure 2-1 Straight Support Standard First Mode Shape.	16
Figure 2-2 Straight Support Standard Third Mode Shape.	17
Figure 2-3 Straight Support Standard Fifth Mode Shape.	18
Figure 2-4 Straight Support Standard Seventh Mode Shape.	19
Figure 2-5 Cantilevered Support Standard First Mode Shape.	20
Figure 2-6 Cantilevered Support Standard Second Mode Shape.	21
Figure 2-7 Cantilevered Support Standard Third Mode Shape.	22
Figure 2-8 Cantilevered Support Standard Fourth Mode Shape.	23
Figure 2-9 Cantilevered Support Standard Fifth Mode Shape.	24
Figure 2-10 Cantilevered Support Standard Sixth Mode Shape.	25
Figure 2-11 Cantilevered Support Standard Seventh Mode Shape.	26
Figure 2-12 Cantilevered Support Standard Eighth Mode Shape.	27
Figure 2-13 S-N Curve for Aluminum.	28
Figure 3-1 Cracked Transformer Base from Route 147.	37
Figure 3-2 Cracked Transformer Base where Shoe Base Bolts on.	37
Figure 3-3 Transformer Base Mounting Procedure.	38
Figure 3-4 Straight Support Standard Positioned for Pull Test.	39

Figure 3-5 Stiffness of Cantilevered Support.	40
Figure 3-6 Natural Frequency of Cantilevered Support.	41
Figure 3-7 Damping of Cantilevered Support with No Damper.	42
Figure 3-8 Damping of Cantilevered Support with Damper.	43
Figure 3-9 Natural Frequency of Straight Support.	44
Figure 3-10 Damping of Motion in Straight Support.	45
Figure 3-11 Linkage to Connect Support Standards in Fatigue Test.	46
Figure 3-12 Actuator Used in Fatigue Test.	46
Figure 3-13 Fatigue Crack in Transformer Base of Specimen S-3.	47
Figure 3-14 Fatigue Crack in Wall of Transformer Base of Specimen S-6	47
Figure 3-15 Cross Section of Transformer Base Wall of Specimen S-6.	48
Figure 3-16 Fatigue Crack in Finger Tabs of Transformer Base of Specimen S-6.	48
Figure 3-17 Large Casting Defect in Transformer Base of Specimen C-6.	49
Figure 3-18 Typical Through-Thickness Weld Toe Crack.	49
Figure 3-19 S-N Curve for Through-Thickness Cracks Not Including the Runouts.	50
Figure 3-20 S-N Curve for Through-Thickness Cracks Including the Runouts.	50
Figure 3-21 Typical Fatigue Crack that Propagates from Behind the Weld Leg.	51
Figure 3-22 Typical Fatigue Crack that Propagates Through the Weld Throat.	51
Figure 3-23 S-N Curve for Shear Stress Range Induced Cracks.	52
Figure 3-24 Striations in Specimen C-4.	52
Figure 3-25 Striations from Cracked Pole on Route 147.	53



# Chapter 1 - Introduction

## 1.1 Problem

Luminaires are used at various locations on major highways and in towns for the purpose of roadway illumination. Luminaire supports come in a variety of configurations and materials. The two most common configurations are a single support with a cantilevered arm and a single, straight support with the light directly on top. Luminaire supports are made from aluminum and from galvanized steel. The cantilevered aluminum luminaire supports that were being researched have the designation of L-8-S-40SB by the New Jersey Department of Transportation (NJDOT) and have a configuration as shown in (Figure 1-1). The straight aluminum luminaire supports that were being researched have the designation of L-E-S-45 by NJDOT and have a configuration as shown in Figure 1-2. These support structures were all manufactured by Hapco and installed by NJDOT.

Recently there were 8 straight and 6 cantilevered luminaire supports that failed along Route 147 in New Jersey. The cantilevered luminaire supports were mounted directly to the parapet of the Grassy Sound Bridge, which is part of Route 147. These cantilevered supports experienced cracking around the shoe base-to-pole weld (Figure 1-3) and at the welds around the hand access holes. The straight poles were used along the side of the road leading up to the bridge. These straight poles were connected to their foundation through the break-away transformer base. All of the poles that were on a transformer base experienced failure through the transformer base (Figure 1-4) and not in the pole or shoe base.

Many other states have reported large amplitude vibrations in their luminaire support standards and in some instances the structures fail. The large amplitude vibration is made possible by the combination of low stiffness and low critical damping ratio in the support structures. These structures have been known to vibrate in both first and second modes. The second mode vibration is believed to be caused by vortex shedding.

The effects of vortex shedding on luminaires were recently studied at the Advanced Technology for Large Structural Systems Engineering Research Center (ATLSS) at Lehigh University for the National Cooperative Highway Research Program (NCHRP). The project was NCHRP 10-38, "Fatigue-Resistance Design of Cantilevered Signal, Sign and Light Supports", which dealt with determining what types of structures would be effected by wind phenomena such as vortex shedding and determining appropriate design fatigue loads for these structures<sup>1</sup>.

## **1.2 Purpose**

The primary purpose of the research described in this report was to determine the fatigue resistance of the socket detail used on the NJDOT luminaire standards and determine what caused the failure of multiple luminaire supports on Route 147 in southern New Jersey. To accomplish this objective 12 luminaire support standards were sent to ATLSS to determine the fatigue resistance of the socket joint at the pole to shoe base connection. Pull tests were also performed to determine the dynamic characteristics, such as stiffness, natural frequency and percent of critical damping of each type of luminaire standard.

## **1.3 Scope**

This report summarizes previous research relevant to the fatigue strength of the socket detail in question. A concrete base was cast to replicate actual foundation conditions of a luminaire standard installed in the field. This base was then used in the fatigue tests and the pull tests. The fatigue testing enabled a decision to be made on the appropriate fatigue strength of the socket connection. Finite element analysis was used to calculate the dynamic characteristics of the luminaire standards. These analytical values were then compared to the measured dynamic characteristics observed during the pull tests.

In addition to this research on the fatigue strength of these poles, a failure analysis was conducted on pieces of the failed poles. The report on this failure analysis was presented previously<sup>15</sup>.

This research was not concerned with determining appropriate mitigation devices for the vibration problems. Mitigation is to be addressed in the phase two studies of NCHRP project 10-38, which are ongoing at the University of Minnesota under the direction of Robert Dexter.

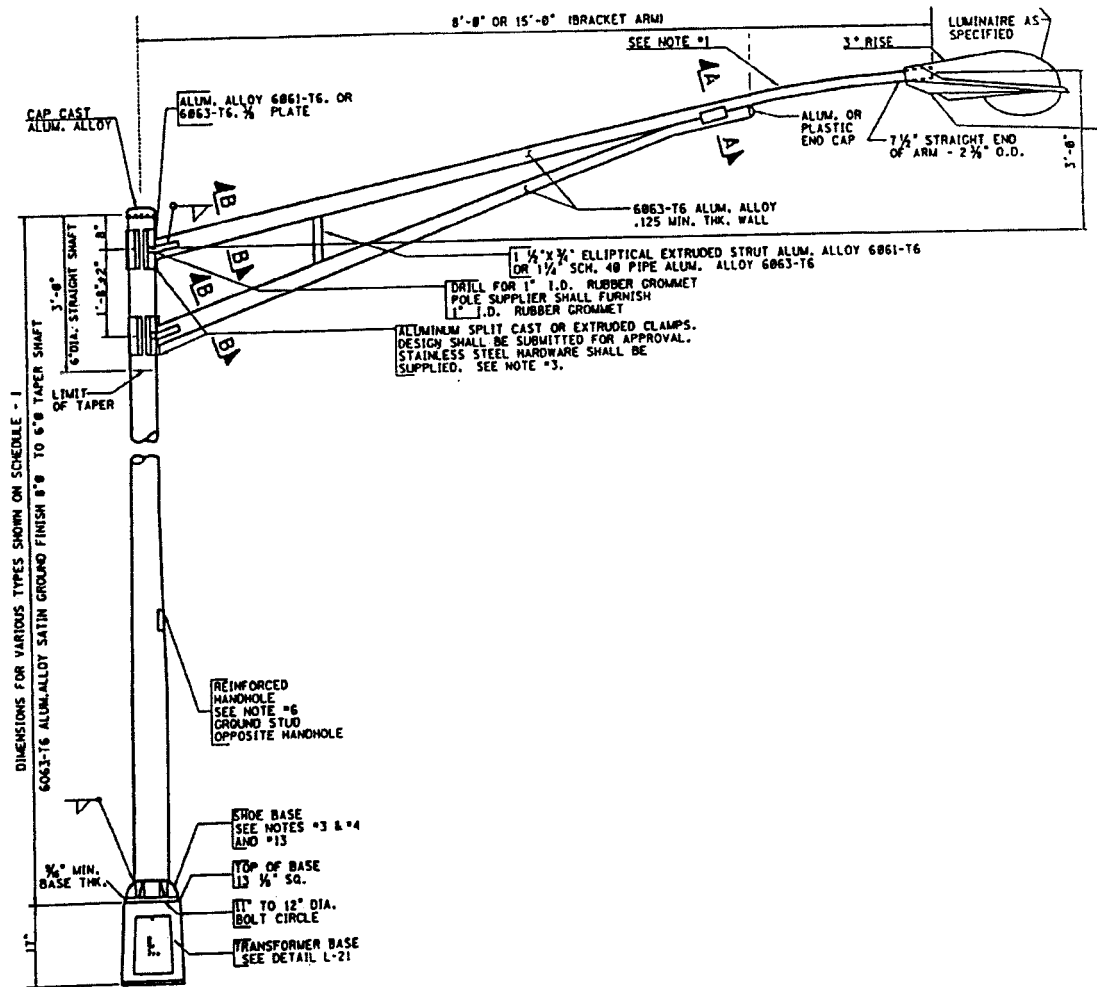


Figure 1-1 Cantilevered Luminaire Support Structure

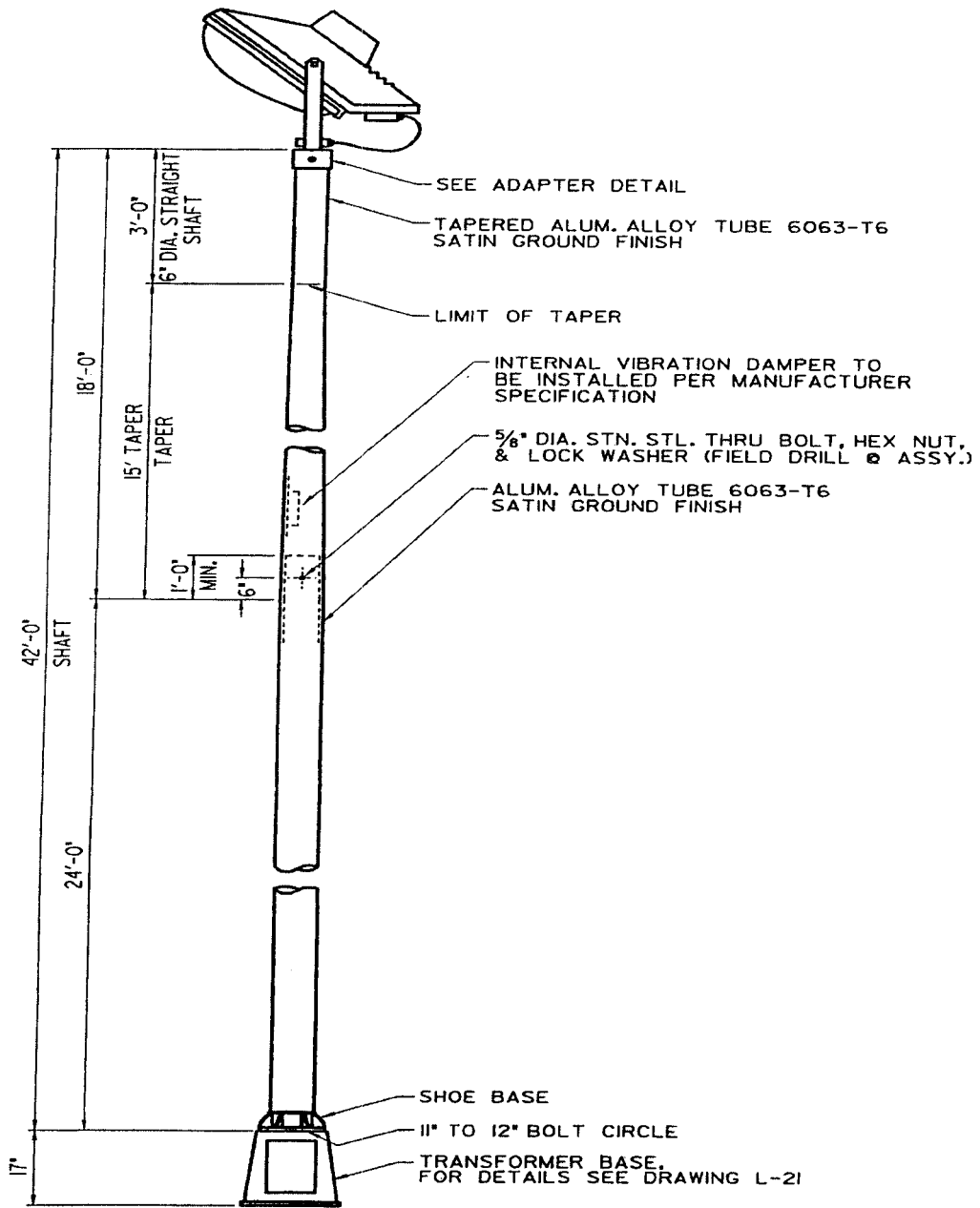


Figure 1-2 Straight Luminaire Support Structure.

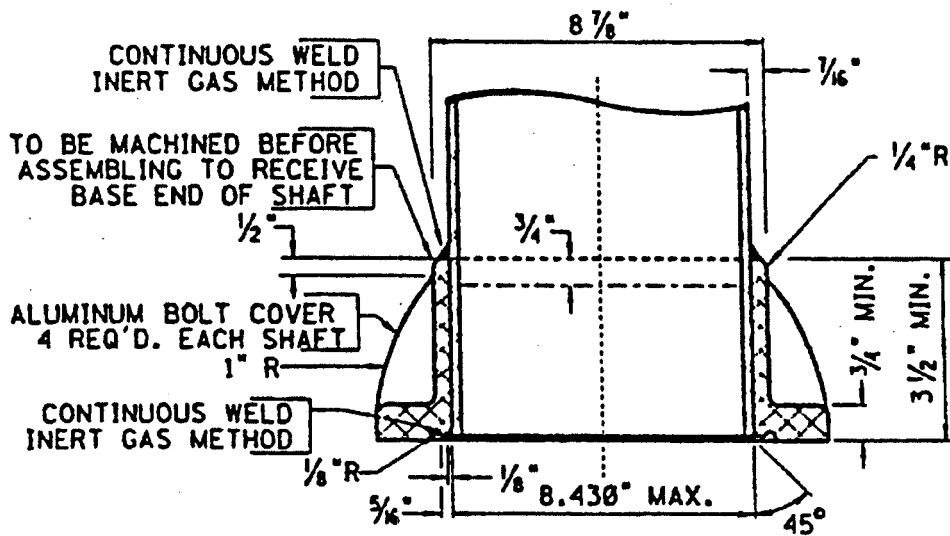
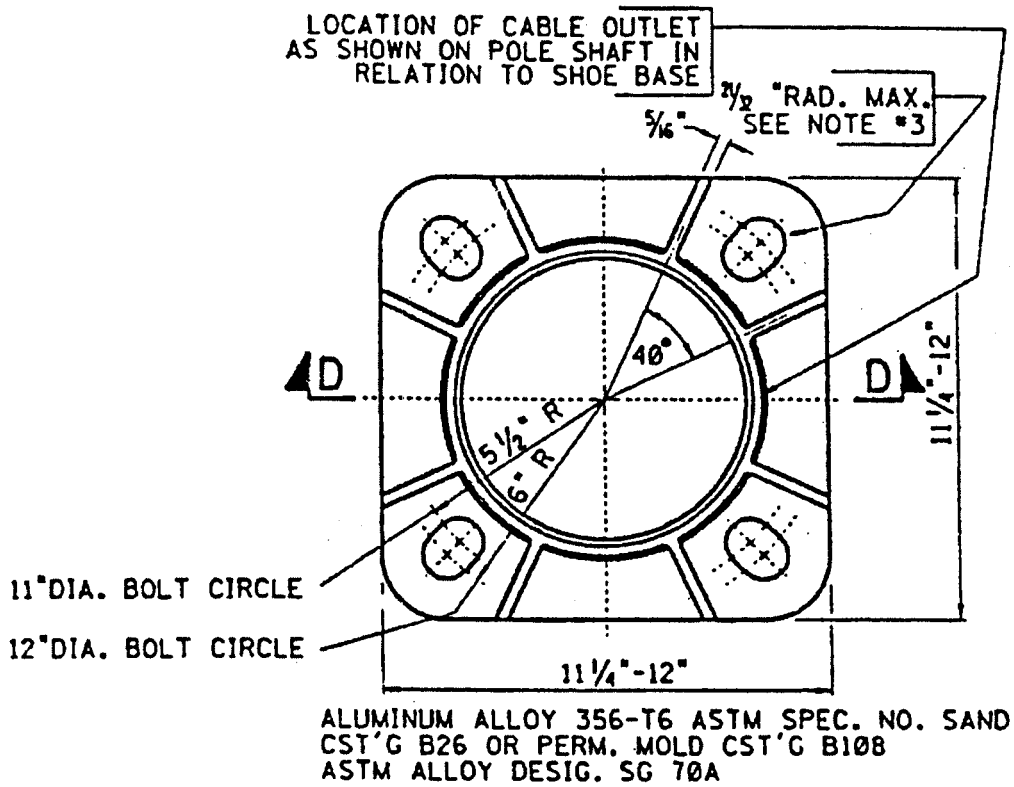


Figure 1-3 Shoe Base to Pole Connection.

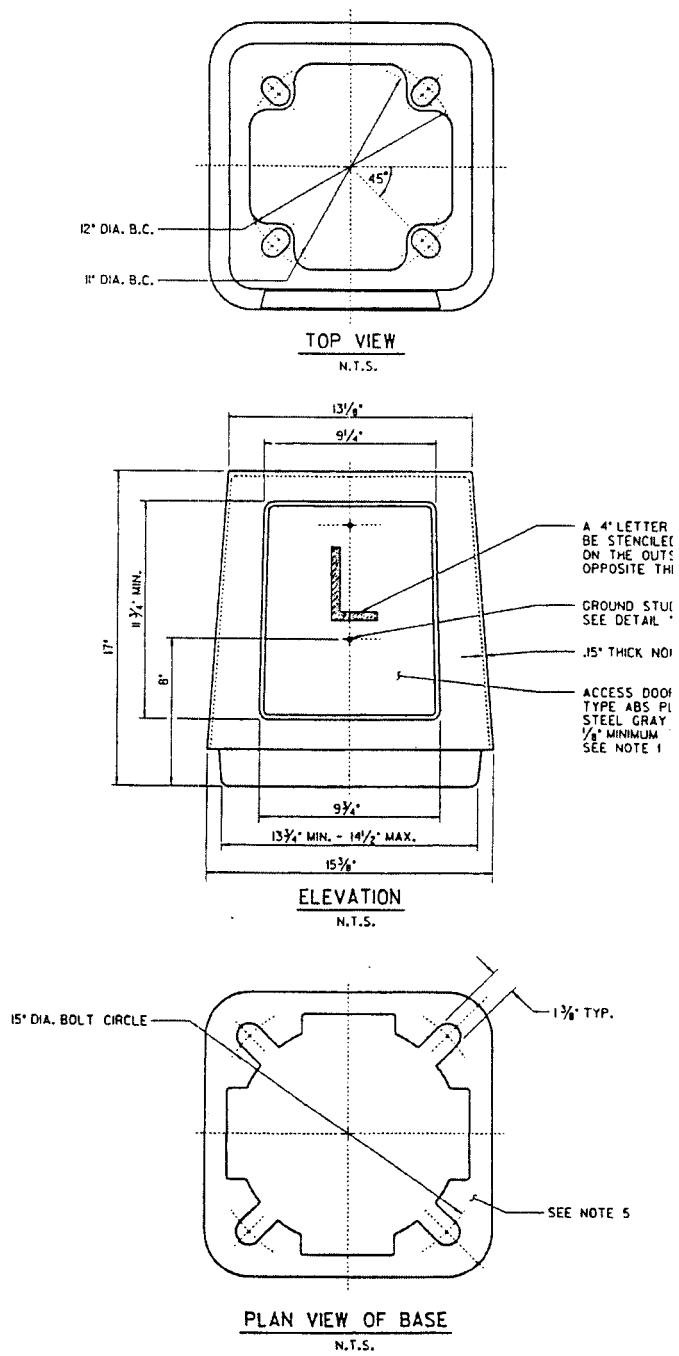


Figure 1-4 Transformer Base.

## **Chapter 2 - Background**

### **2.1 Wind Loading Phenomena Relevant to Luminaires**

Luminaire supports are susceptible to two wind phenomena, natural wind gusts and vortex shedding. All structures are susceptible to natural wind gusts. Vortex shedding is a problem for luminaire supports because their shape enables the formation of uniform vortices to form around the structure.

#### **2.1.1 Natural Wind Gusts**

The response of typical cantilevered support structures to natural wind gusts was modeled using spectral finite-element analysis. The structure is broken up into several continuous areas such as signs or exposed portions of the structure. The fluctuating wind force on each area and the resulting response variables (such as column base moment) during a short interval are characterized as stationary random processes. The response spectrum can be related back to the expected variable-amplitude history of the response as a function of time. Specifically, the root-mean-square (RMS) of the random response time history is found from the integration of the response spectrum over all significant frequencies. In the case of luminaire support structures, there are only a few significant frequencies, therefore the integration is performed by simply summing the response at these frequencies.

The wind force spectrum is derived from the velocity spectrum. A standard wind velocity spectrum (which depends on the mean hourly wind velocity) was selected from the literature <sup>2</sup>:

$$S_v(f) = \frac{4KV_{10}^2 x^2}{f(1+x^2)^{4/3}} \quad (2-1)$$

where  $S_v(f)$  is the spectral density of the velocity (which has units of velocity squared multiplied by time),  $f$  is the cyclic frequency (cps),  $K$  is a terrain coefficient (m/s)<sup>2</sup>,  $V_{10}$  is the mean wind velocity (m/s) at a reference height of 10 meters, and  $x$  is the quantity (1200 meters \*  $f$ )/ $V_{10}$  (dimensionless for  $V_{10}$  in m/s). The terrain coefficient  $K$  was taken as 0.005 which is typical for open grassy terrain <sup>2,3</sup>.

The drag force is proportional to the square of the velocity and both the force and the velocity can be represented as the sum of their mean and fluctuating components. Through algebraic manipulation of these relationships, the following relations can be obtained <sup>3</sup>:

$$\left(\frac{d}{v}\right)^2 = \frac{4 D^2}{V^2} = 4 C^2 A^2 V^2 \quad (2-2)$$

where  $d$  and  $D$  are the fluctuating and mean value of the drag force respectively,  $v$  and  $V$  are the fluctuating and mean value of the wind velocity respectively,  $A$  is the total frontal area of the surface which is causing the drag, and  $C$  is a constant equal to  $0.5rC_d$  with  $r$  equal to the density of air and  $C_d$  equal to the drag force coefficient. The density was taken as  $1.22 \text{ kg/m}^3$  which is the value for "standard air" (one atmosphere pressure at  $14^\circ\text{C}$ ).

The force and velocity spectra are proportional to the square of the fluctuating components of force or velocity, therefore the ratio of these spectra is equal to the ratio in Equation 2-3, i.e.:

$$S_F(f) = 4 C^2 A^2 V^2 S_v(f) \quad (2-3)$$

The force spectrum must be calculated for the total frontal area of a surface and cannot be broken down into sub-areas. One spectrum is calculated for each luminaire attachment. Additional spectra are calculated for each continuous exposed portion of the cantilevered arm or pole. These spectra must be completely correlated to each other in the analysis.

Important assumptions must be made regarding: 1) the mean wind velocity at which the support structures should be analyzed; and, 2) estimating the effective stress range from the RMS of the variable amplitude response. It is impractical to forecast the future wind history at each location for luminaire support structures. Therefore, some very simple assumptions were made. The design procedure is based on a spectral analysis using the mean hourly wind velocity, which was exceeded in only 0.01 percent of all hours. It is accepted that the probability of exceedence of mean hourly wind velocity at a location is a Rayleigh distribution, which depends only on the yearly mean wind velocity  $V_m$ , i.e.:

$$P_E(v) = e^{-\frac{\pi v^2}{4V_m^2}} \quad (2-4)$$

where  $P_E(v)$  is the probability that a randomly-occurring mean hourly velocity is greater than the velocity magnitude  $v$  and  $e$  is the base of the natural logarithms. The limit-state mean hourly velocity is found by setting  $P_E$  equal to 0.01 percent and solving for  $v$ .

The yearly mean wind velocity also varies from place to place. A collection of yearly mean wind speed data from weather stations at 59 cities across the U.S. was examined. Most weather stations are located at airports, therefore the data should be representative of most open terrain. The data showed that 81 percent of the cities had a mean wind velocity at 10 m (33 ft) above the ground less than 5 m/s (11 mph). It was decided to use 5 m/s (11 mph), which was exceeded in only 19 percent of U.S. cities, as the baseline case for a static design pressure in the specifications. The mean hourly wind velocity for this yearly mean wind speed is 17 m/s (37 mph).

The result of the analysis, the spectral density of the response, has units of the response (such as moment or stress) squared multiplied by time. When the spectral density of the response is integrated across a range of frequencies, the result (the area



under the spectrum) is equivalent to the variance of the response about the mean. The square-root of this area is the root-mean-square (RMS) of the response. The time history of the response is narrow-banded (concentrated about one frequency), since the response is still dominated by the resonant frequency. For random, narrow-band time histories, the average or effective stress range  $S_r^{eff}$  can be estimated from the relationship which gives the stress range for a constant-amplitude response in terms of the RMS of the stress response  $\sigma_{rms}$ <sup>5</sup>, i.e.:

$$S_r^{eff} = 2.8 \sigma_{rms} \quad (2-5)$$

A variety of sign, signal, and luminaire support structures were analyzed at a mean wind velocity of 17 m/s and values of normalized equivalent static pressures for these structures ranged from 170 to 300 Pa (3.6 to 6.3 psf). Considering the numerous uncertainties in this analysis, not enough is known to assign greater or lesser loads to different types of structures. Also, separate loading for different types of structures would unnecessarily complicate the design process. Therefore, these values were averaged and rounded to 250 Pa (5.2 psf), which is recommended for design. This natural wind gust pressure must be applied to a variety of surfaces with widely varying drag coefficients. Therefore the recommended static design pressure must be multiplied by the appropriate drag coefficient and then may be applied to the surface. The structures should be designed so that the stress ranges resulting from the application of this load range are below the constant amplitude fatigue limit (CAFL)<sup>1</sup>.

These calculations indicate that most structures will eventually be susceptible to cracking from natural wind gusts, but the recommended loads are not so large as to predict rapid failure. These results are consistent with observed service fatigue failures that can be attributed to natural wind gusts. Because of the uncertainty in these assumptions, the recommended equivalent static load range can be easily adjusted for other mean wind speeds.

### **2.1.2 Vortex Shedding**

Vortex shedding typically develops during steady, uniform flows, and produces resonant oscillations in a plane normal to the direction of flow. Vortex shedding is caused by the shedding of vortices in a regular, alternating pattern in the wake of a structural element. The phenomenon has been observed in a wide-range of structures, including chimneys, hyperbolic cooling towers, antenna masts, and pipelines.

When a structural element is exposed to a steady, uniform flow, vortices are shed in the wake behind the element in an alternating pattern commonly referred to as a Von Karman vortex street. The frequency at which vortices are shed from the element,  $f_s$ , is given by the Strouhal relation:

$$f_s = \frac{SV}{D} \quad (2-6)$$

where  $S$  is the Strouhal number,  $D$  is the across-wind dimension of the element, and  $V$  is the free-stream wind velocity. As is indicated by Equation 2-6, the frequency at which vortices are shed is dependent upon the velocity of the flow, the across-wind dimension of the element, and the shape of the element (as defined by the magnitude of the Strouhal number). The Strouhal number for a luminaire with a round cross section, or with the same geometry as the poles on Route 147, is 0.18.

When the frequency of vortex shedding, as predicted by the Strouhal relation, does not match one of the natural frequencies of the structure, the shedding of vortices in the wake of a structure will elicit only a nominal periodic response. However, when the frequency of vortex shedding approaches one of the natural frequencies of a flexible, lightly-damped structure, significant displacement ranges and stress ranges can result. The across-wind resonant vibration has a strong organizing effect on the pattern with which vortices are shed. The result is an increase in vortex strength, an increase in the spanwise correlation of the vortex shedding forces, and a tendency for the vortex shedding frequency to become coupled to the natural frequency of the structure. This phenomenon is called "lock-in". The critical wind velocity,  $V_{cr}$ , at which lock-in occurs is given by the Strouhal relation:

$$V_{cr} = \frac{f_n D}{S} \quad (2-7)$$

where  $f_n$  is the natural frequency of the structure. The result is a condition of resonant vibration that persists over a range of wind velocities.

The amplitudes of vibration associated with the lock-in phenomenon are generally limited by the ability of vortices to be shed from the structure in a symmetric pattern. Large amplitudes of vibration tend to interfere with the symmetric pattern of vortex formation. Previous research indicates that the maximum amplitudes of displacements associated with the lock-in phenomenon rarely exceed approximately 1 to 1.5 times the across-wind dimension of the structural element from which vortices are shed<sup>6,7</sup>.

The fact that uniform steady-state flow is required for vortex shedding can be used to bound the velocities under which various elements of luminaire support standards could possibly be susceptible to vortex-induced vibrations. Previous research indicates that the level of turbulence associated with wind velocities above approximately 15 to 20 m/s (35 to 45 mph) limits the symmetric formation of periodic vortices<sup>7</sup>. Also, vortex formation at wind velocities below approximately 5 m/s (10 mph) generates forces with magnitudes insufficient to excite most structures. Based upon this knowledge, structures may be susceptible to vortex-induced vibrations in the range of wind velocities between approximately 5 and 15 m/s (10 to 35 mph).

### **2.1.2.1 Straight Support Standards Susceptibility to Vortex Shedding**

Before describing the susceptibility to vortex shedding of the different mode shapes of the luminaire support standards the definition of the mode numbers needs to

be clarified. There is often a difference between the actual mode number and what is often referred to as "second mode" and "third mode". These later terms are commonly used to describe the groups of modes that put the poles into double or triple curvature, respectively. This report will use the actual mode number because it is the correct one.

Although there has been evidence in the past that vortex shedding is not a problem for most types of highway support structures it is believed to have played a potential role in the failure of the luminaire support standards along Route 147. Due to the dynamic characteristics of most highway support structures, vortex induced vibration is not typical in the first mode because the critical wind velocity is below 5 m/s. As was explained above this will generate a force with insufficient magnitude to excite the structure. First mode vibration is where most of the experimental data has been carried out on these types of structures. Higher modes may occur at frequencies that would be more conducive to vortex-induced vibrations. Table 2-1 is a summary of the first four modes of the straight support standard along Route 147. The critical velocities were calculated using Equation 2-7. Because the straight support standard is perfectly symmetric the mode shapes come in pairs for a three dimensional analysis. In other words, the first and second mode shapes are the same, the third and fourth are the same, and so on, therefore only every other mode number is discussed. Figure 2-1 shows the first mode shape of the straight support standard. As can be seen in Table 2-1 this mode would not be induced by vortex shedding because the critical wind velocity is too low.

Figure 2-2 and Figure 2-3 shows the third and fifth mode shape respectively. As can be seen in Table 2-1, the third and fifth mode shapes both have a critical velocity that is in the range that is conducive to vortex shedding. Figure 2-4 shows the straight support standard in the seventh mode shape. Table 2-1 shows that this mode would likely not occur due to vortex shedding because the critical velocity is too high.

<b>Mode Shape</b>	<b>Natural Frequency</b>	<b>Critical Velocity (m/s)</b>
1	0.74*	0.7
3	5.24	5.2
5	15.2	15.0
7	29.9	29.5

\*Based on experimental data from pull tests, all others are based on FEA.

Hapco manufactures a damper that helps to stop second mode vibration. This damper is supposed to be standard on the 45 ft. straight support standards that were used along Route 147. Hapco has done testing on this damper by attaching it to a support standard mounted to a rigid foundation. Calculations showed that the percent of critical damping with and without the damper installed increased from 0.18% to 0.83% respectively. This amount of damping would probably increase in an actual luminaire support standard due to a less rigid base and the wires inside flapping

around. Hapco estimates that the percent of critical damping with the damper installed could increase to 2.5%, however this number is not based on results from experimental testing of an actual luminaire support standard on a foundation in second mode vibration.<sup>8</sup>

It is not clear how this damper will effect third mode vibration. As was discussed above, third mode vibration, in the straight support standard, is possible through vortex shedding. According to eyewitness reports by NJDOT there have been support standards that take on a third mode shape in the field. This could have been the mode that took place in the straight support standards along Route 147. It is impossible to say because no one was present to witness the supports just before failure.

### **2.1.2.2 Cantilevered Support Standards Susceptibility to Vortex Shedding**

As was explained above, first mode vibration of the cantilevered support standards would probably not be induced by vortex shedding because the critical wind velocity is too low. Higher modes of vibration could occur however due to their higher natural frequency causing a higher critical wind velocity. Table 2-2 is a summary of the first six modes of the cantilevered support standards along Route 147. The critical velocities were calculated using Equation 2-7. Figure 2-5 shows the first mode shape of the cantilevered support standards. As can be seen in Table 2-2 this mode would not be induced by vortex shedding because the critical wind velocity is too low. The first mode of the cantilevered support standard is a twisting of the pole due to the eccentric mass of the luminaire and self-weight of the mast arm. This type of motion would probably not cause the necessary stress ranges to cause a crack at the shoe base to pole connection anyway.

Figure 2-6 and Figure 2-7 shows the second and third mode shapes of the cantilevered support standard, respectively. As can be seen in Table 2-2 these modes would not be induced by vortex shedding because their critical velocities are also too low.

Figure 2-8 shows the fourth mode shape of the cantilevered support standard. The critical wind velocity for the fourth mode shape to occur is a little low, however there have been reports from NJDOT that have suggested this mode shape has been witnessed in the field. Figure 2-9, 2-10 and 2-11 show the fifth, sixth and seventh mode shapes of the cantilevered support standard, respectively. As can be seen in Table 2-2 these mode shapes require a critical wind velocity that is capable of causing vortex-induced vibrations. As can be seen by comparing Figure 2-8 to Figure 2-10 the mode shapes for mode four and six are very similar. A slight double curvature of the pole in mode six is what distinguishes the two. It would be very easy for someone in the field to mistake mode four for mode six. Realizing this, it is probably unlikely that mode four was witnessed in the field as was reported by NJDOT. Considering the required critical wind velocity of mode four and mode six, it is more likely that the support standards were vibrating in mode six.

Figure 2-12 shows the eighth mode shape of the cantilevered support standard. As can be seen in Table 2-2 this mode shape has gone beyond the range for the critical wind velocity necessary for vortex shedding.

Mode Shape	Natural Frequency	Critical Velocity (m/s)
1	0.79	0.7
2	1.02*	0.9
3	1.7	1.5
4	3.9	3.5
5	7.2	7.1
6	7.5	7.4
7	10.1	10
8	16.1	15.9

Dampers are not supplied as standard items on the 40 ft. cantilevered luminaire support standards that were installed along Route 147. These particular cantilevered support standards can be outfitted with an external damper if they appear to exhibit excessive vibrations. Reports from both Hapco and NJDOT indicate that some of the cantilevered support standards along Route 147 did not have dampers installed on them at the time of the failure. These support standards would have been susceptible to any of the modes of vibration, whether due to vortex shedding or some other phenomenon that could induce vibration.

The excessive vibration of the support standards on the bridge could have been induced by the bridge itself. Support standards that are mounted on bridges have been known to exhibit excessive vibration that is induced by the bridge they are mounted to, particularly if the vibration of the bridge is in tune with one of the natural frequencies of the support standards. However, since there were also failures of poles that were not mounted to the bridge, it is unlikely that this is the primary cause of these failures. Installing a damper on any support standard that will be mounted to a bridge, no matter what the geometry of the support standard, would probably be worthwhile.

### **2.1.2.3 Recommended Vortex Shedding Design Loads**

The current AASHTO Standard Specification for Structural Supports for Highway Signs, Luminaires, and Traffic Signals, 1994 only addresses the first mode of a non-tapered structural member for fatigue loads related to vortex shedding<sup>9</sup>. The methods that are used for this circumstance are correct and are applicable to the specific geometry described above. However, as has been discussed throughout this report, the susceptibility to vortex shedding goes beyond the first mode. In some

cases the first mode occurs at a critical wind velocity that is not conducive to vortex shedding anyway. It is necessary to calculate design loads for modes beyond the first. The Ontario Highway Bridge Design Code (OHBDC) gives an in-depth description of vortex shedding in different modes of vibration<sup>10</sup>. OHBDC also discusses the appropriate changes in the fatigue loads when a tapered pole is used. This code is quite complex and may be more involved than is actually needed to satisfactorily design a luminaire support standard.

## **2.2 Background Relevant to Fatigue Resistance of Details**

Fatigue cracks can form and propagate from weld discontinuities and/or stress concentrations if a member is subjected to significant cyclic live loads, even if the maximum stresses are well below the yield strength<sup>11, 12</sup>. Testing on full-scale welded aluminum members has indicated that the primary effect of constant amplitude loading can be accounted for in the live-load stress range, i.e. the mean stress is not significant. The reason that the dead load has little effect on the lower bound of the results is that, locally, there are very high residual stresses in welded details. Therefore, the mean of the total stresses (applied plus residual stresses) is relatively high regardless of the dead load. In details that are not welded, such as anchor bolts, there is a strong mean stress effect. A worst-case conservative assumption, i.e. a high tensile mean stress, is made in the testing and in the design of these nonwelded details.

When structural members are tested, the loading is characterized in terms of the nominal stress in the structural member remote from the weld detail. The local stress concentration effect associated with the shape of the weld is considered part of the fatigue resistance. The nominal stress is conveniently obtained from standard design equations using member forces and moments from a global analysis.

Experience with multiaxial loading experiments on large-scale welded aluminum structural details indicates the loading perpendicular to the local notch or the weld toe dominates the fatigue life. The cyclic stress in the other direction has no effect if the stress range is below 83 MPa (12 ksi) and only a small influence above 83 MPa (12 ksi). Since the combination of multiaxial loading does not have to be considered. The recommended approach for multiaxial loads is:

- 1) decide which loading (primary or secondary) dominates the fatigue cracking problem (typically the loading perpendicular to the weld axis or perpendicular to where cracks have previously occurred in similar details); and,
- 2) perform the fatigue analysis using the stress range in this direction (i.e. ignore the stresses in the orthogonal directions)<sup>11</sup>.

The strength and type of aluminum have only a negligible effect on the fatigue resistance expected for a particular detail. The welding process also does not typically have an effect on the fatigue resistance. The independence of the fatigue resistance from the type of aluminum greatly simplifies the development of design rules for fatigue since it eliminates the need to generate data for every type of aluminum.

Aluminum fatigue test data generally consist of the number of cycles to failure for a particular detail subjected to a particular constant amplitude stress range. The results are in general highly variable, therefore a statistically significant number of replicate tests must be performed. The large variance in the number of cycles to failure is primarily due to variance in both the weld geometry and weld discontinuities. This large variance makes it difficult to distinguish the secondary effects of many variables such as type of aluminum and filler metal, rate of loading, mean stress, and the environment.

Fatigue tests are performed at a number of different stress ranges and the data are generally plotted with the logarithm of the nominal stress range on the ordinate and the logarithm of the number of cycles to failure on the abscissa (even though the number of cycles is the dependent variable). The relationship used to represent the lower bound to aluminum detail test data is referred to as an S-N curve (Figure 2-13). An S-N curve is an exponential equation of the form:

$$N = C \times S^{-m} \quad (2-8)$$

or

$$\log N = \log C - m \log S$$

where  $N$  is the number of cycles to failure,  $C$  is the constant dependent on detail category,  $S$  is the applied constant amplitude stress range, and  $m$  is the inverse of the slope of the S-N curve.

Figure 2-13 shows the constant amplitude fatigue limits (CAFL) of aluminum for each category as horizontal dashed lines. When constant amplitude tests are performed at stress ranges below the CAFL, noticeable cracking does not occur. Luminaire support structures experience what is known as long-life variable-amplitude loading, i.e. very large numbers of random amplitude cycles greater than the number of cycles associated with the CAFL. In this case, the fatigue design consists of making sure that the upper bound stress range, as defined by the recommended fatigue design load ranges, is less than the CAFL. If this is true, then the fatigue life should be essentially infinite.

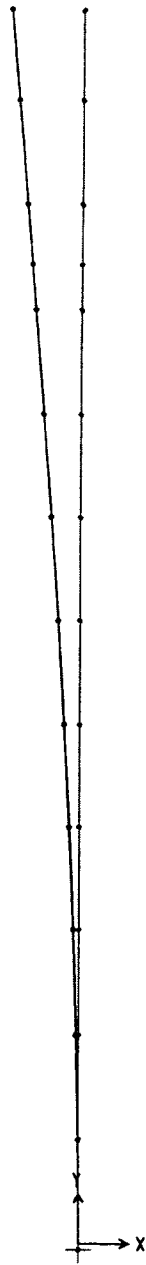


Figure 2-1 Straight Support Standard First Mode Shape.





Figure 2-2 Straight Support Standard Third Mode Shape.



Figure 2-3 Straight Support Standard Fifth Mode Shape.

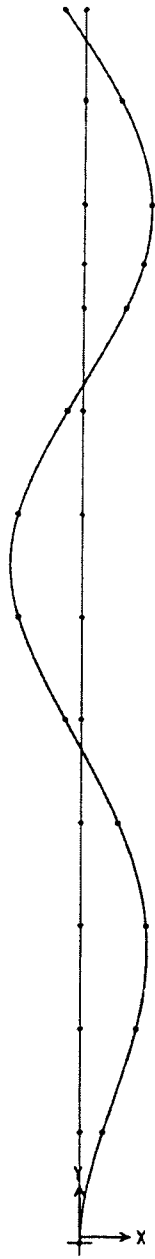


Figure 2-4 Straight Support Standard Seventh Mode Shape.

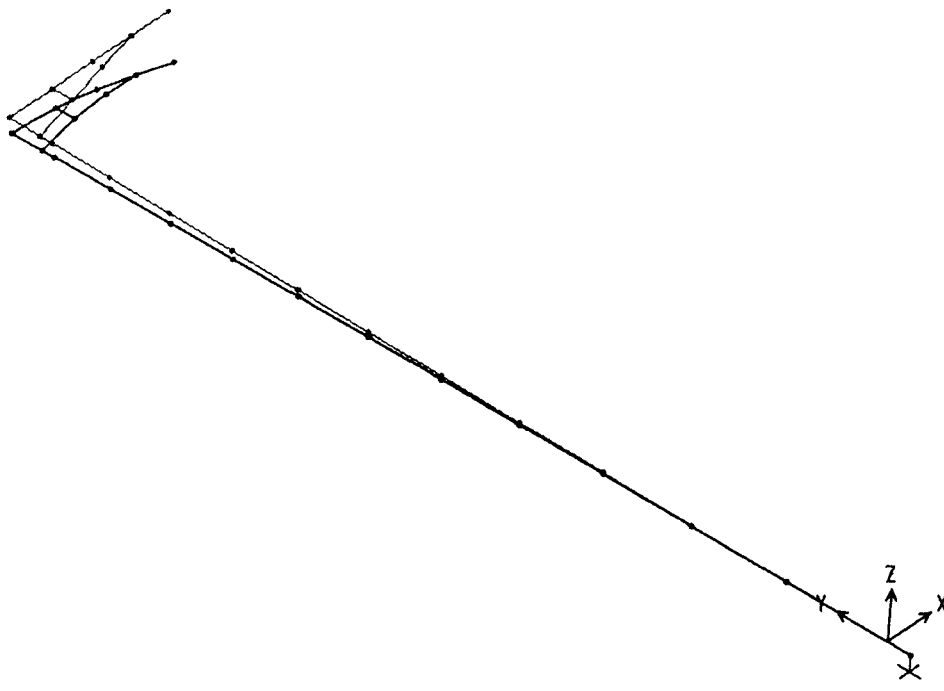


Figure 2-5 Cantilevered Support Standard First Mode Shape.

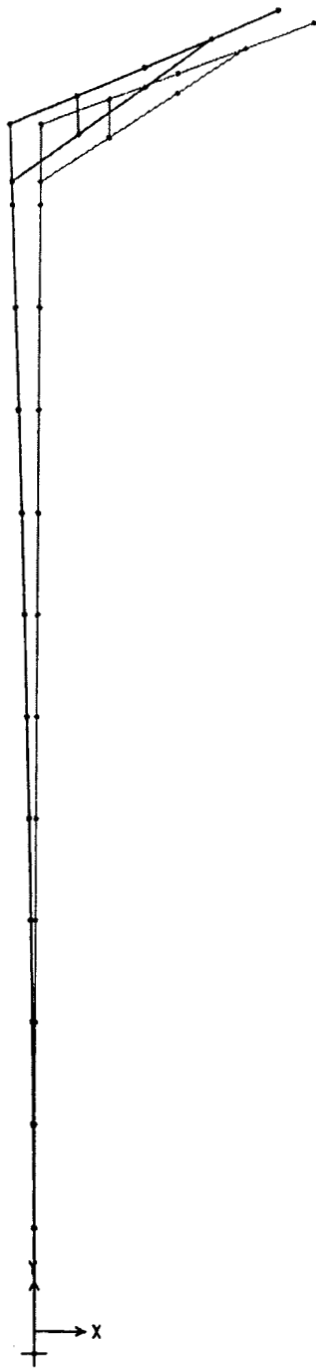


Figure 2-6 Cantilevered Support Standard Second Mode Shape.

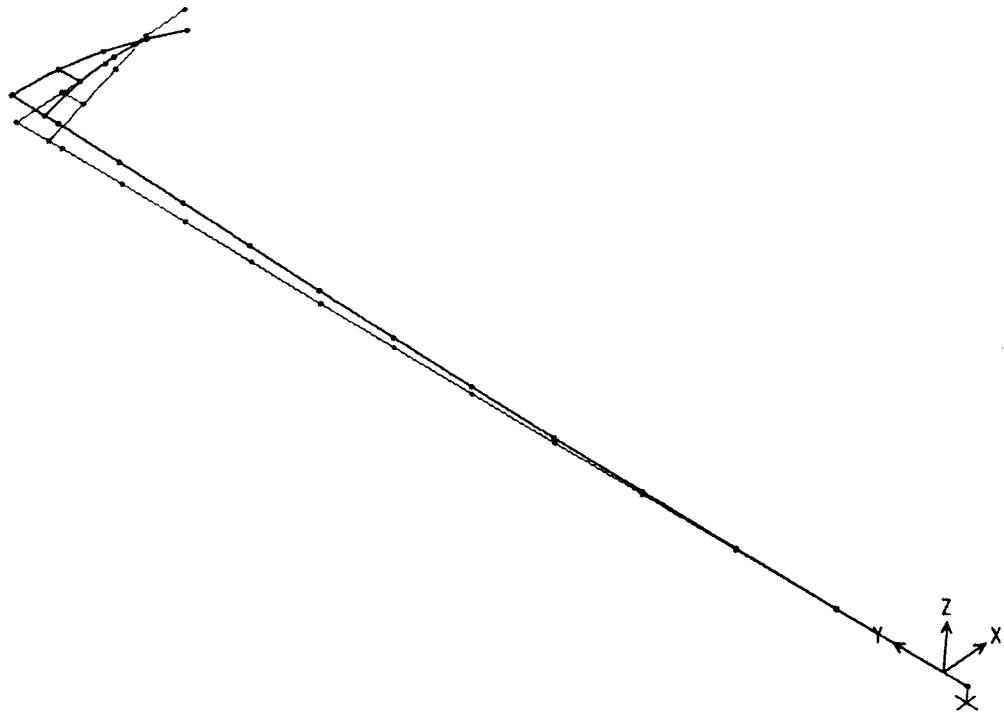


Figure 2-7 Cantilevered Support Standard Third Mode Shape.

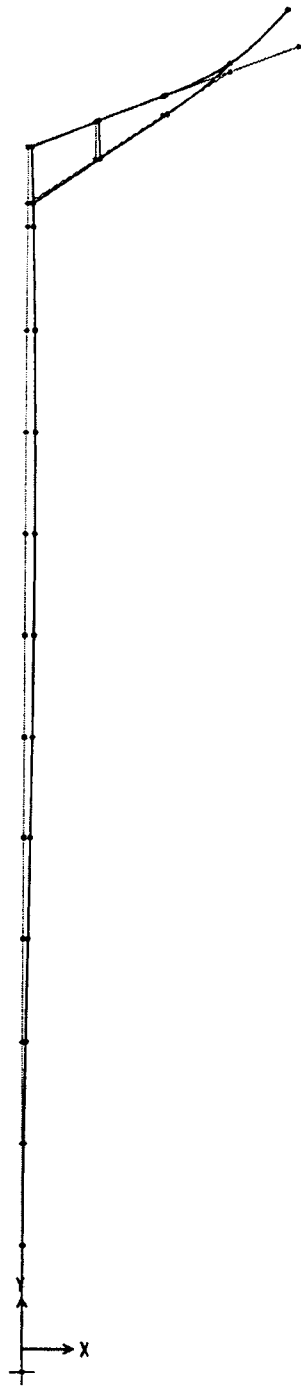


Figure 2-8 Cantilevered Support Standard Fourth Mode Shape.

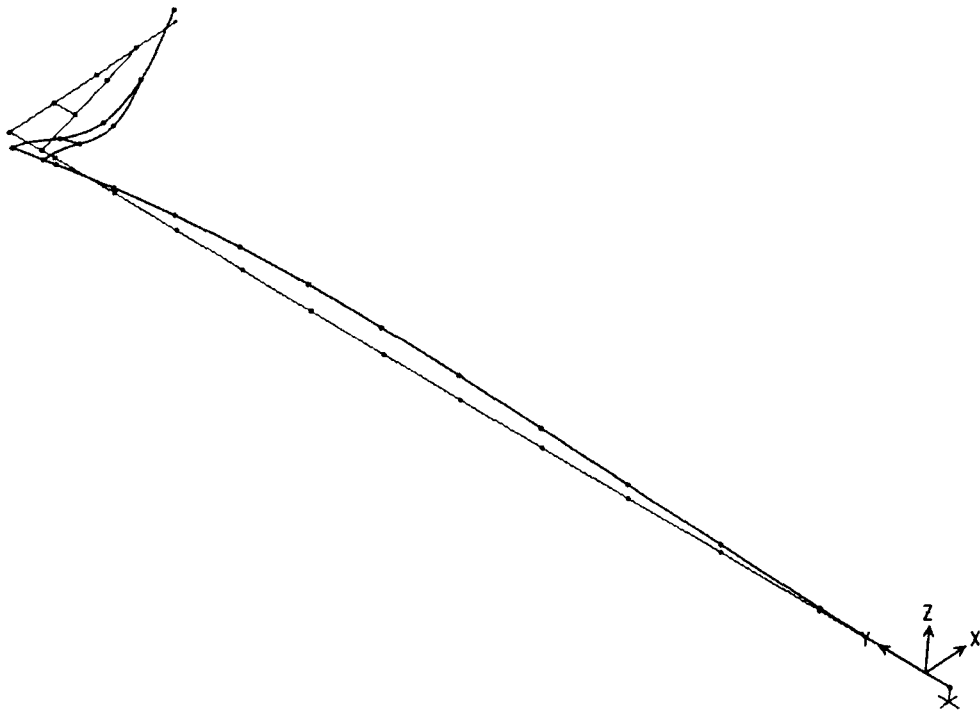


Figure 2-9 Cantilevered Support Standard Fifth Mode Shape.



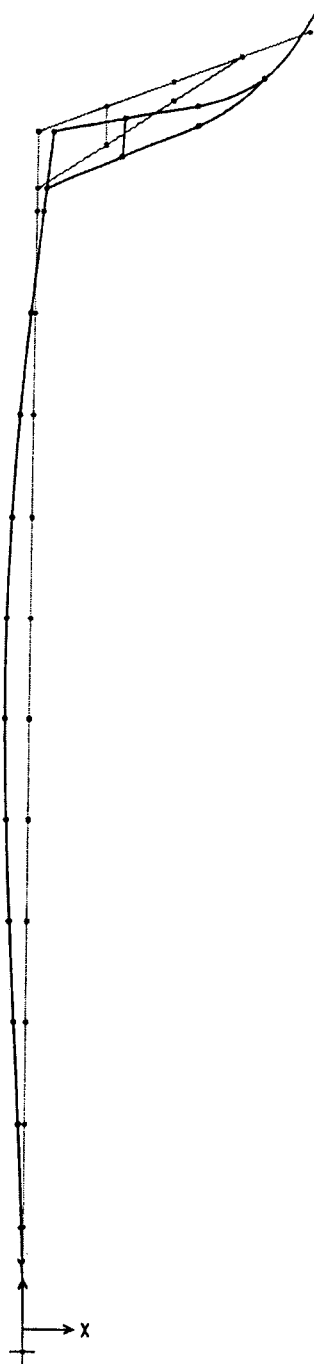


Figure 2-10 Cantilevered Support Standard Sixth Mode Shape.

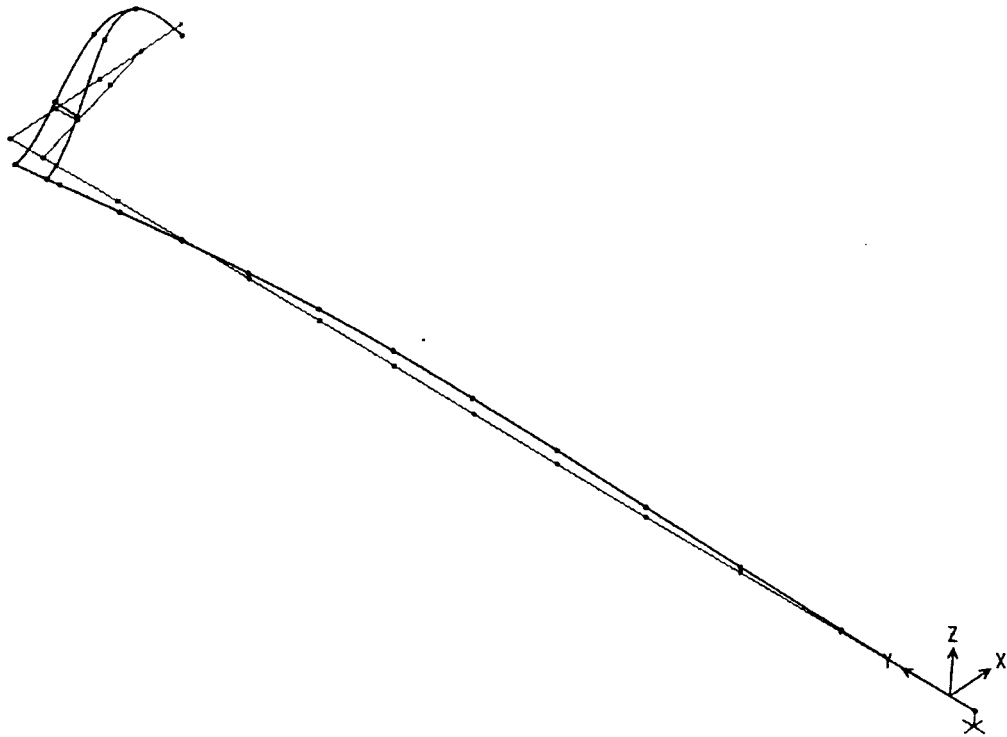


Figure 2-11 Cantilevered Support Standard Seventh Mode Shape.

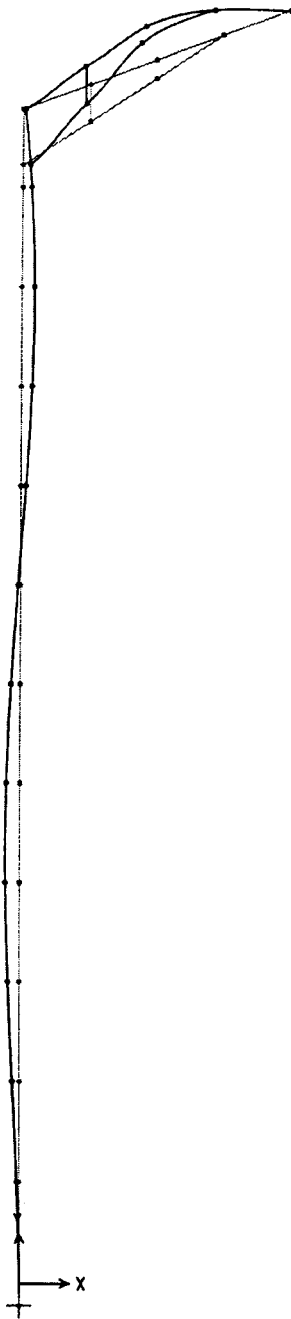


Figure 2-12 Cantilevered Support Standard Eighth Mode Shape.

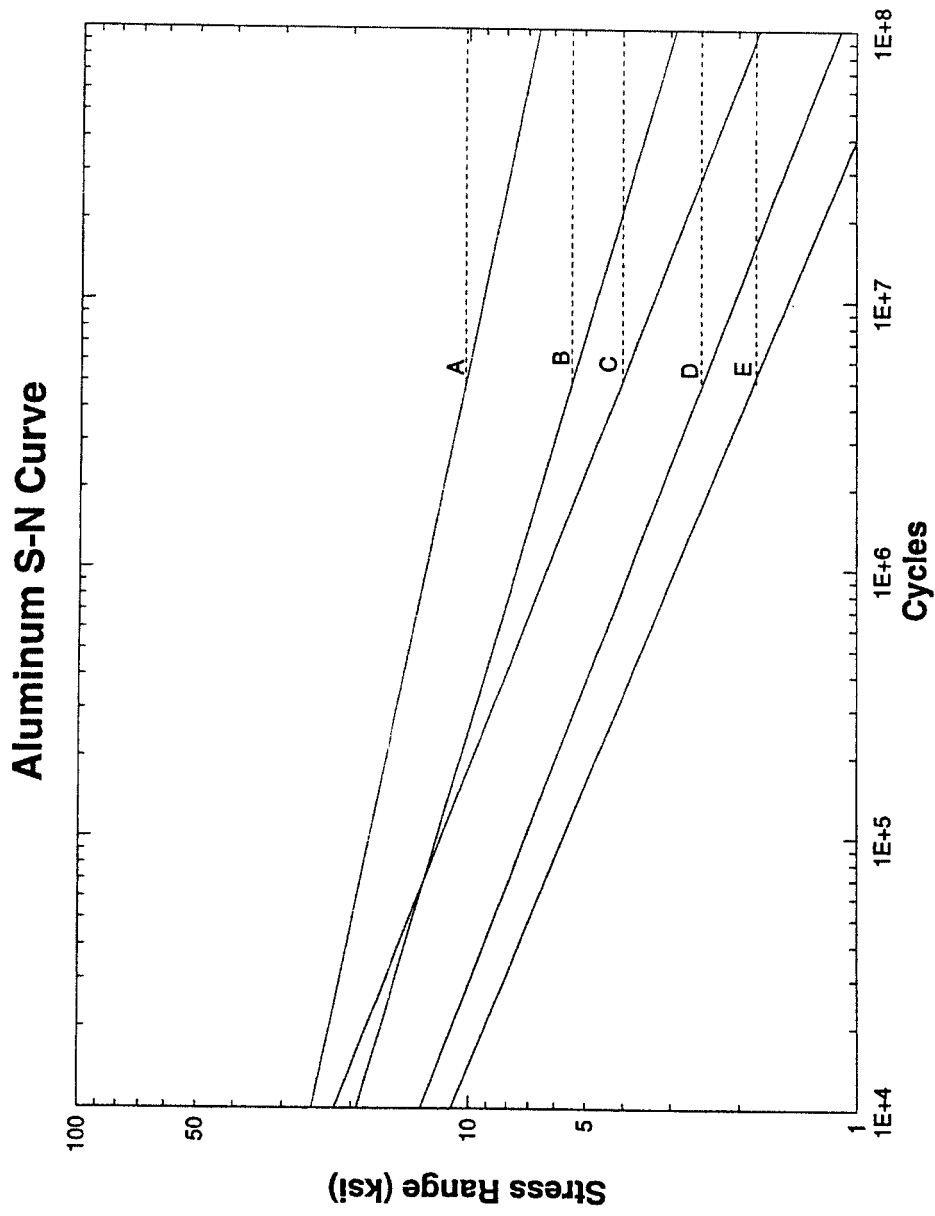


Figure 2-13 S-N Curves for Aluminum.

## **Chapter 3 – Testing and Findings**

### **3.1 History of the New Jersey Luminaire Support Standards**

The aluminum luminaire support standards that failed were located in southern New Jersey on Route 147. The cantilevered support standards were mounted directly to the parapet of the Grassy Sound Bridge, which is part of Route 147. These support standards experienced cracking around the shoe base-to-pole weld and at the welds around the hand access holes. The straight support standards were used along the side of the road leading up to the bridge. Only the straight support standards were connected to their foundation through the break away transformer base. All of the poles that were on a transformer base experienced failure through the transformer base and not in the pole or shoe base.

Figure 3-1 is a transformer base that was cracked alongside Route 147. In the event of an impact by a motorist, these bases are intended to break off at the tabs on the bottom where they bolt to their foundation. These breakaway tabs would seem to be the location of some of the failures since they are designed to be the weak link in the transformer base, however none of the bases appeared to fracture there. A video of the failure site taken by Hapco the next morning provided a means to view some of the failures<sup>14</sup>.

The videotape was a valuable tool in examining the failures. Many of the cracks in the transformer bases occurred at the top where the shoe base bolted on (Figure 3-2). This may have been partly due to an error at the time the support standards were erected. Figure 3-3 describes the proper hardware, as specified by the manufacturer, to install the transformer bases. In many cases the heavy half-inch thick galvanized steel washer that helps to stiffen the transformer base around the long-slotted bolt holes were not installed. According to Hapco this leads to approximately a 50% reduction in the strength of the transformer base.

A second observation from the videotape was the lack of any significant oxidation at any of the failure surfaces. This would tend to indicate that the fatigue cracks had not been present for too long before failure occurred. A fractographic examination of a failed shoe base and transformer base indicated that the cracks did grow at a very high rate after initiation<sup>15</sup>.

It is suspected that the support standards may have entered a mode of vibration other than first mode on the night of their failures. It was reported by Hapco and NJDOT that many of the cantilevered support standards did not have a damper installed on them. Dampers are only standard on the 45 ft. straight support standards; the other support standards are fitted with dampers only if they exhibit excessive vibrations. These dampers have only been proven effective on the second mode of vibration of a straight support standard and may have not had any effect if a higher mode of vibration were achieved.

### **3.2 Pull Test Description**

A pull test was performed on both the cantilevered and straight luminaire support standards to determine the dynamic characteristics such as stiffness, natural frequency, and percent of critical damping

Figure 3-4 shows a straight support standard that has been positioned for a pull test. A rope was looped around the support 34 ft. up from the shoe base, which was just below the bottom part of the mast arm on the cantilevered support standards. The rope was looped around in a manner that would allow it to fall off the support standard when released so as not to add any additional damping to the system. The rope was hooked to a quick release device to allow an almost instantaneous release of the support standard. The support standard was ratcheted back by a come-along that was connected to a rigid frame. A small load cell was calibrated and placed between the come-along and quick release device. A string pot was connected to the specimen at the same location the load was applied. The string pot was disconnected from the support standard before being released with the quick release mechanism, so as not to add any additional damping to the system. With the combination of load from the load cell and deflection from the string pot a stiffness for the system could be calculated. Strain gages were attached to the support standard so a decay of motion could be recorded. A natural frequency can be extracted from the strain gage data by performing a Fast Fourier Transform (FFT).

#### **3.2.1 Cantilevered Support Standards Pull Test Results**

The pull test enabled the dynamic characteristics, such as the stiffness, natural frequency, and percent of critical damping to be calculated. Figure 3-5 shows a plot of load versus displacement. Based on this plot a stiffness of 3.6 N/mm can be calculated. A finite element analysis gives a stiffness of 3.4 N/mm. This is an excellent agreement between the FEM model and experimental data.

A Fast Fourier Transform was performed on data from a strain gage while the support standard oscillated at its second mode natural frequency. As was mentioned before, the first mode of the cantilevered support standards is twisting of the pole and is not relevant to fatigue. The natural frequency in the second mode was 1.02 cycles/s (Figure 3-6). Finite element analysis indicated a second mode frequency of 1.04 cycles/s. As with the stiffness this is an excellent agreement.

The log-decrement equation, Equation 3-1, was used to determine the percent of critical damping in the support structure

$$\frac{1}{j} \ln \frac{u_1}{u_{1+j}} = \frac{2\pi\zeta}{\sqrt{1-\zeta^2}} \quad (3-1)$$

where  $j$  is the number of cycles being considered,  $u_1$  is the amplitude at peak 1,  $u_{1+j}$  is the amplitude  $j$  cycles later, and  $\zeta$  is the damping ratio. The percent of critical





















































•

•

•

•

•

•

•

•

•

























